5-2013

Exploration into Properties of Molybdenum Disulfide using Atomistic Simulation

Joseph Simpson
University of Arkansas, Fayetteville

Exploration into Properties of Molybdenum Disulfide using Atomistic Simulation

An Undergraduate Honors College Thesis

in the

Department of Mechanical Engineering
College of Engineering
University of Arkansas
Fayetteville, AR

by

Joseph P. Simpson

This thesis is approved.

Thesis Advisor:

DOUGLAS SPEAROT

Thesis Committee:

DOUGLAS SPEAROT

Exploration into Properties of Molybdenum Disulfide using Atomistic Simulation

Joseph Simpson
Department of Mechanical Engineering, University of Arkansas, Fayetteville, AR

Molybdenum disulfide (MoS_2) has a lamellar crystal structure, which makes it ideal for use as a solid lubricant. Transmission electron microscope (TEM) images have shown that line defects exist within the lattice of mechanically deformed MoS_2, but the physical mechanisms which lead to the formation of these defects are unknown. The two central objectives of this research are to use molecular dynamics simulations to study the effects of tensile deformation on both single layer and bulk MoS_2 and explore the properties of line defects in an otherwise perfect lattice of MoS_2. Under tensile loading, molecular dynamics simulations show a multi-stage stress versus strain diagram. Atomistic visualization shows a distinct change in the structure of the lattice during tensile stretching. This new structure is likely the result of a phase transformation. For the second objective, a series of computational approaches are used to create a single line defect in a perfect MoS_2 lattice. Shearing both parallel and perpendicular to the basal plane of MoS_2 and compression leading to buckling were unsuccessful in moving the line defect.

1.0 Introduction:

Molybdenum disulfide, or MoS_2, is an inorganic compound that has a layered hexagonal crystalline structure. Each layer in this crystalline structure consists of alternating sheets of Sulfur - Molybdenum - Sulfur. There are two different prevalent bonds that are present in the lattice of MoS_2, covalent interatomic bonds and van der Waals bonds. The covalent interatomic bonds hold together the individual sheets of sulfur and molybdenum that compose a single layer of MoS_2 and the van der Waals bonds hold each of the layers together. Together, these bonds

form a lamellar, or stacked, structure. The van der Waals bonds are considerably weaker and break easily during a shearing force. If a shearing force is applied to MoS_2, the van der Waals bonds are the first to break, allowing the layers to slide parallel to each other, however they also provide the cushion that creates the extremely low friction coefficient. These van der Waals bonds allow for a relatively high load to be applied perpendicular to the lattice while still allowing for the layers to easily slide parallel to each other [2]. For this reason, MoS_2 can operate standalone as a solid lubricant or as an additive to liquid lubricants which can not only increase wear resistance, but also reduce the friction coefficient.

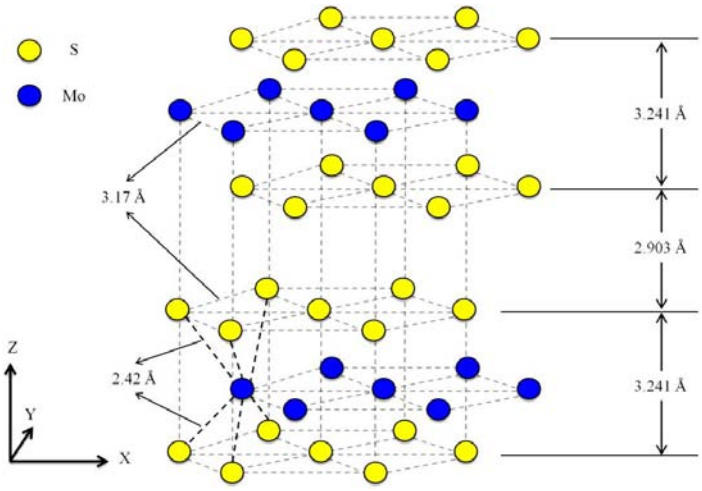

Figure 1. Crystal Structure of MoS2. [1]

As a standalone solid lubricant, it is useful in space applications where suspension in liquids becomes ineffective. Molybdenum disulfide can retain a low friction coefficient in temperatures up to 600 degrees Fahrenheit in oxygen rich environments [4]. After the temperature reaches 600 °F, the MoS_2 oxidizes and forms molybdenum trioxide (MoO_3) and sulfur dioxide (SO_2) [4]. In an oxygen deficient environment, such as space, MoS_2 not only excels due to its molecular properties, but also in the fact that it can reach temperatures of up to 1300 °F [4]. MoS_2 is frequently used as an additive

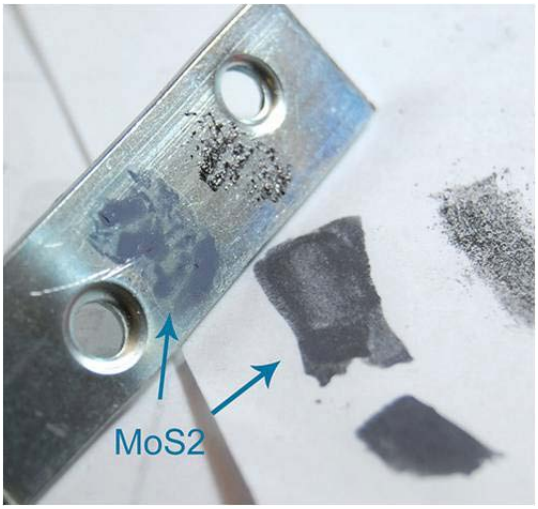

Figure 2. Comparison of MoS2 and Graphite after suspension in an alcohol solution. [3]

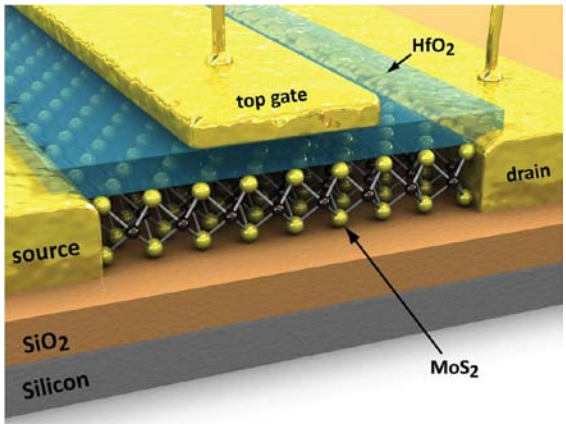

Figure 3. MoS2 used in place of traditional silicon in a transistor. [6]

to liquid lubricants to improve lubrication properties [4]. Another use that has garnered recent popularity is single layer MoS_2 as a substitute for silicon in micro electronics. The limitations of silicon are mainly the minimum size, around 2 nanometers thick, that it can reach before it starts to oxidize. A single layer of molybdenum disulfide, which is 0.65 nanometers thick, is gaining popularity as a potential solution to the problem produced as electronics continue to push the extremely small size. Not only can molybdenum disulfide be used to create smaller electronics, but it can also be used to make transistors that consume up to 100,000 times less energy than it's silicon counterparts [5].

Although there were many avenues explored in this research, all of them led toward two central objectives: studying the effects of tensile deformation on both single layer and bulk MoS_2, and exploring the properties of line defects in an otherwise perfect lattice of MoS_2. The first central objective, studying the effects of tensile deformation on both single layer and bulk MoS_2, was divided into many parts, or tasks. The first task was to find suitable boundary conditions for the simulations such that there would be no boundary interference during simulations. Once suitable boundary conditions had been found, the next tasks were (1) to study effects of temperature variation of the stress-strain response under biaxial tension, (2) to study the role of lattice thickness on the stress-strain response of MoS_2 under biaxial tension, and (3) to study the stress-strain response of a single layer of MoS_2 under uniaxial tension. The last task deals with the exploring the region with the "plateau" in the single layer stress-strain under uniaxial tension and correlating those critical points with physical deformation of the lattice.

Next was the second central objective, exploring properties of line defects in an otherwise perfect lattice of MoS_2. The initial tasks that needed to be completed before any research into defects could be conducted were: creating an MoS_2 lattice with correct placement and properties and introduction of a line defect in the perfect lattice of MoS_2. Both of these objectives had to be completed in such a way that was both repeatable and reasonable with regards to applications of MoS_2. After these initial objectives were completed, research could then be performed into the interaction of the defect with the surrounding lattice and the mobility of the defect in the lattice.

2.0 Background:

Prior to the introduction of computers, research was classified into either experimental or theoretical. The experimental research provided results from a system subjected to certain measurements and criteria. The theoretical research involved constructing a system, usually using sets of mathematical equations, that was verified or validated by its ability to accurately describe the behavior of a system in a few cases. These theoretical systems, or models, could only be easily validated under a few special circumstances. This was a problem due to the fact that most of the more intriguing problems did not fall in the area of these special circumstances. This gap between experimental and theoretical research was bridged with the introduction of high speed computers. The computers created a new form of research that is in the middle of the existing two called the "computer experiment" [7]. This new form employs models provided by the theorists and calculations performed by the computers which led to a theoretical experiment that also produced results. Due to the fact that it was a combination of the two former types of research, results of the computer experiment would also need to be validated against

experimental results. The computer experiment opened up a vast expanse of possibilities in computational research that is related to almost every aspect of life today [7].

There are many different types of computational methods employed to perform various simulations. These can range from atomic simulation, which focuses on the atomic scale, to finite element analysis, which can be used to model large scale simulations such as automobile impacts. This research into various properties of molybdenum disulfide was performed using a form of atomistic simulation called molecular dynamics [7].

Molecular dynamics is a computer simulation technique that allows for the analysis of physical movements of atoms and molecules. In other words, molecular dynamics uses high speed computers to solve the classical equations for motion, in the simplest case Newton's Second Law of Motion $F = ma$, for each atom in the system. Molecular dynamics requires three basic elements to perform simulations. First, it requires information on how each atom will interact with the other atoms in the system, known as interatomic potentials. Secondly, it needs a procedure to numerically integrate the equations of motion. Finally, molecular dynamics needs initial conditions for the atoms in the system, which would include velocities and positions [7].

A set of interatomic potentials is one of the three basic elements needed by molecular dynamics to perform atomistic simulations. Due to the structure of molybdenum disulfide, two separate interatomic potentials were required; one potential to model the covalent bonds in each individual S-Mo-S layer and one potential to model the van der Waals bonds between S-Mo-S layers. The first potential that was used was a reactive empirical bond order potential (REBO). A reactive empirical bonder order potential allows for the fracture and formation of bonds to occur over the course of the simulation. The REBO potential is an excellent fit for these molecular dynamics simulations due to the fact that it not only is able to yield a good agreement

with the "structure and energetics" of the MoS_2 components, but also because the path of the research involves exploration into defect interaction including both fracture and formation of bonds over the course of the simulation [8]. The equation for the reactive empirical bond order given by Liang *et al.* [8] is expressed as,

$$E_{REBO} = \frac{1}{2}\sum_{i\neq k} f_{ij}^{c}(r_{ij})\left[V^{R}(r_{ij}) - b_{ij}V^{A}(r_{ij})\right]$$

$$= \frac{1}{2}\sum_{i\neq k} f_{ij}^{c}(r_{ij})\left[\left(1 + \frac{Q_{ij}}{r_{ij}}\right)A_{ij}e^{-\alpha_{ij}r_{ij}} - b_{ij}B_{ij}e^{-\beta_{ij}r_{ij}}\right],$$

where r_{ij} is the distance of separation between atoms *i* and *j*, $f_{ij}^{c}(r_{ij})$ is the cutoff function, $V^{R}(r_{ij})$ and $V^{A}(r_{ij})$ are the repulsive and attractive interactions, respectively, and b_{ij} is the many-body bond order function [1].

The second potential used for molybdenum disulfide is a Lennard-Jones potential. As the REBO potential characterizes the interactions between the atoms in the individual layers, the Lennard-Jones potential characterizes the interactions between the layers of MoS_2. The Lennard-Jones potential used for these simulations is a common 12-6 potential given by the expression

$$\emptyset_{LJ}(r) = 4\varepsilon\left[\left(\frac{\sigma}{r}\right)^{12} - \left(\frac{\sigma}{r}\right)^{6}\right]$$

where ε and σ represent the LJ parameters for each pair of atoms. The first term in the brackets, $\left(\frac{\sigma}{r}\right)^{12}$, becomes the dominant component at shorter distances. It models the repulsive force that occurs when the atoms are brought close to each other. The second term in the brackets, $\left(\frac{\sigma}{r}\right)^{6}$, becomes the dominant component at larger distances. This second term models the attractive forces and is the term that gives a cohesion to the system. This potential accurately models the

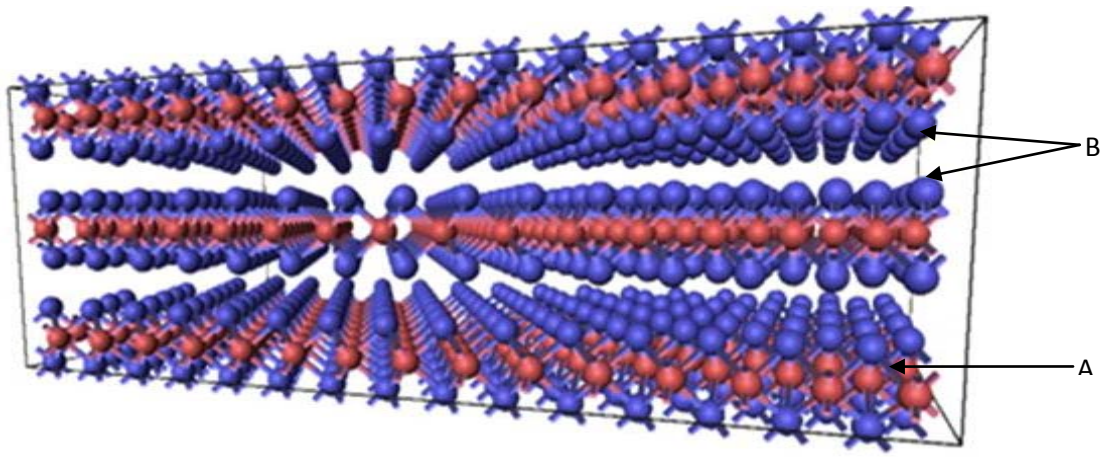

Figure 4. Lattice of MoS2. A) The interatomic bonds modeled by the REBO. These bonds are very strong compared to B) the van der Waals bonds modeled by the Lennard-Jones potential.

interatomic forces between the layers and also gives an explanation as to its low friction properties. The attractive force of the second term holds the layers together in a lamellar structure. As a force is applied, the layers of the lattice compress. When this happens, the first term takes over and the repulsive force becomes dominant, forcing the layers apart in the way two magnets repel each other. If there is sufficient tangential force applied to the system, the layers will slide parallel to each other. The van der Waals bonds, modeled by the Lenard-Jones potential, are the origin of the low frictional properties and its popular use as a solid lubricant [7].

In molecular dynamics, there are many different scenarios under which simulations are run. These different scenarios provide different sets of equations for the simulation based on which ensemble is chosen. For instance, an NPT molecular ensemble maintains a constant number of atoms, system pressure, and system temperature with a variable volume, while an NVT molecular ensemble maintains a constant number of atoms, system volume, and system temperature with a variable pressure. Other ensembles include NPH, which maintain constant number of atoms, system pressure, and system enthalpy, and NVE, which maintains a constant number of atoms, system volume, and system energy which is accompanied by a temperature

rescaling command.. This command allows for the use of an NVE ensemble while maintaining a constant temperature. This research uses a combination of the NVE, NVT, and NPT ensembles. The NPT ensemble, for example, was used in the case of pure uniaxial strain, allowing the width of the system to change in response to the length placed under tension [9]. Boundary conditions are a serious consideration when running simulations. There are two types of boundary conditions used in this research, periodic and non-periodic. Periodic boundary conditions create a system that continues infinitely in the direction of the axis that is chosen. It does this by virtually copying the current simulation cell and pasting it on either side [9]. This is important because if the system is too small, the boundary conditions will interfere with and alter the simulation. An example of periodic boundary conditions and the role of boundary conditions on a system can be seen in Figure 5. In the image above, the red lines and arrows show the path of a phase change throughout a lattice of MoS_2. This helps visualize periodic boundary conditions and how it allows researchers simulate larger systems using smaller simulation cells. Part of this research went into finding appropriate boundary conditions for simulations to negate any interference from the boundaries on the system. A simple example can show the importance of

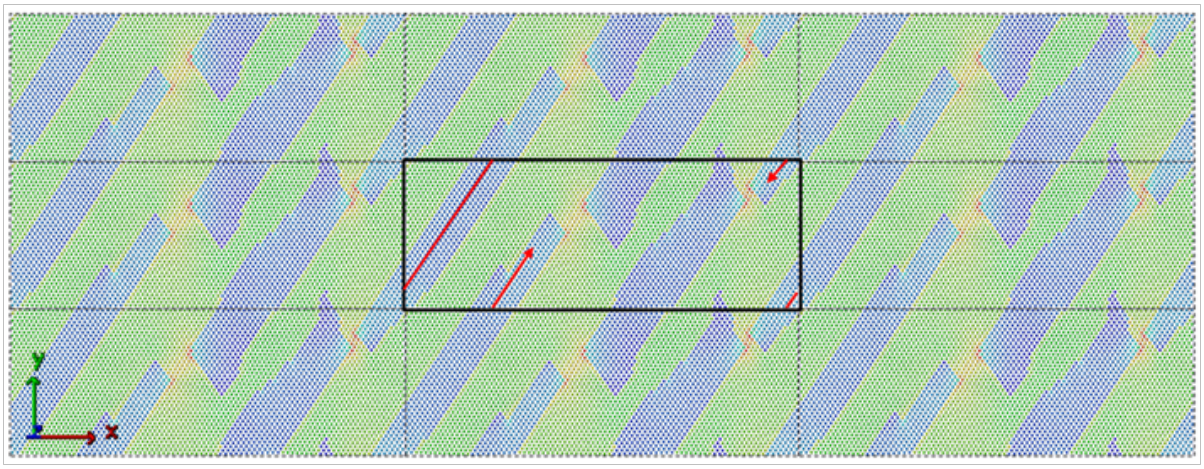

Figure 5. Top view of a single sheet of MoS2. The center box with the bolded outline is the original simulation cell and the outer boxes are representative of periodic boundary conditions.

boundary conditions. If a simulation was run of a nano-indentation with a simulation cell that did not have an adequate size, a round indenter may be partially cut off. This would result in a configuration similar to Figure 6. Although it is an exaggerated example, it shows the importance of choosing proper boundary conditions. Non-periodic boundary conditions simply create an edge to the simulation box. In Figure 6, there are periodic boundary conditions in the y-direction and non-periodic boundary conditions in the x-direction. Different simulations call for different configurations of periodic and non-periodic boundary conditions. Simulations for single layer MoS_2, for example, should have periodic boundary conditions in the x and y directions, as shown in Figure 5, but non-periodic boundary conditions would be optimum in the z direction, which is the thickness of the system.

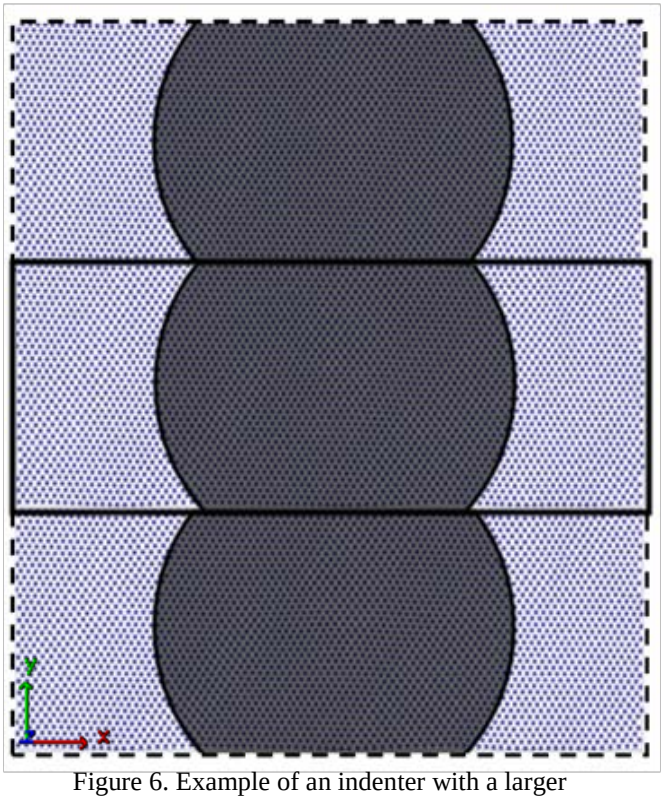

Figure 6. Example of an indenter with a larger radius than the width of the sheet of MoS2 and its effects on periodic boundary conditions.

The simulations performed for this research were done using the classical molecular dynamics code called LAMMPS. LAMMPS is an acronym for Large-scale Atomic/Molecular Massively Parallel Simulator. LAMMPS is a free, open source MD code that is distributed by Sandia National Laboratories [10]. For this research, the LAMMPS package was installed and run on both the STAR and RAZOR supercomputers located at the University of Arkansas. Altogether, the Arkansas High Performance Computing Center has 4,985 core which equates to

13.4 terabytes of memory, approximately 73 teraflops/s CPU peak performance, and 93 terabytes of long term storage [11]. The simulation process starts when the written code is submitted to the supercomputing queue. When it reaches the top of the queue, the supercomputer runs the code and writes the bulk of the information processed to two types of files, log and dump files. The log files give a record of the simulations that were performed during the duration of the run and has all of the numerical information used to analyze the system. The dump files contain all of the information that is used to visualize the simulation. It can include numerous things from the basic positions of atoms to evaluations of potential energies of each atom. The next step is to open the dump file in a program called OVITO. OVITO is open source software developed by Alexander Stukowski for the purpose of analysis and visualization of atomistic simulations [12]. OVITO takes the dump file and inputs the positions and properties of the atoms at each time step, giving a visualization of what happens during the course of the simulation [12]. The steps above are the basic process that is used in all simulations throughout this research.

3.0 Description of the Research

The first obstacle in performing this research was becoming proficient with both the LAMMPS code and its functionality. In order for most users to overcome this obstacle, LAMMPS has several built in examples that are meant to be altered in order to aid in the learning process. These initial, built in, examples were comprised of nickel. The benefit of the built in LAMMPS examples were that new users were taught the main commands, which remained the same regardless of which material is defined.

3.1 Effects of Tensile Deformation on Single Layer and Bulk MoS_2

The first lattice of molybdenum disulfide was constructed after conversing with James Stewart, a graduate student in Microelectronics and Photonics Graduate Program, who provided both the Lennard-Jones and REBO potentials. An interesting observation about the first lattice that was created was the fact that the atoms were vibrating relative to each other. This phenomena was caused by the system not being in thermal equilibrium. There were two steps taken to alleviate this problem. First, an energy minimization step was added directly after the creation of the MoS_2 lattice. This energy minimization step takes every atom in the system and attempts to put it in the lowest energy state possible. This also corrects any possible mistakes that might have occurred in the creation of the lattice. After adding this energy minimization, the layers began to vibrate as a whole with respect to the neighboring layers. The next step was running a small equilibration step to bring the system into a thermal equilibrium.

Now that the lattice had been created with the correct potentials and properties, the next step was finding the appropriate boundary conditions to accurately run the simulations. The original lattice that was constructed was not acceptable to perform the simulations involving defects due to its size. If the lattice was too small, the defect in the center of the lattice would be greatly impacted by the boundary conditions. If the lattice was increased to a much larger size then needed, it would produce an unwarranted strain on the supercomputers that are used by numerous other researchers. To optimize the size of the system, simulations were run on a series of different lattice sizes to find the most appropriate simulation size. For this research the x, y, and z directions represent the length, width, and thickness, respectively. The loading techniques for the initial exploration into size for the length, width, and height involved a rigid region on either end of the lattice. These regions remained rigid and fixed unless otherwise specified. This

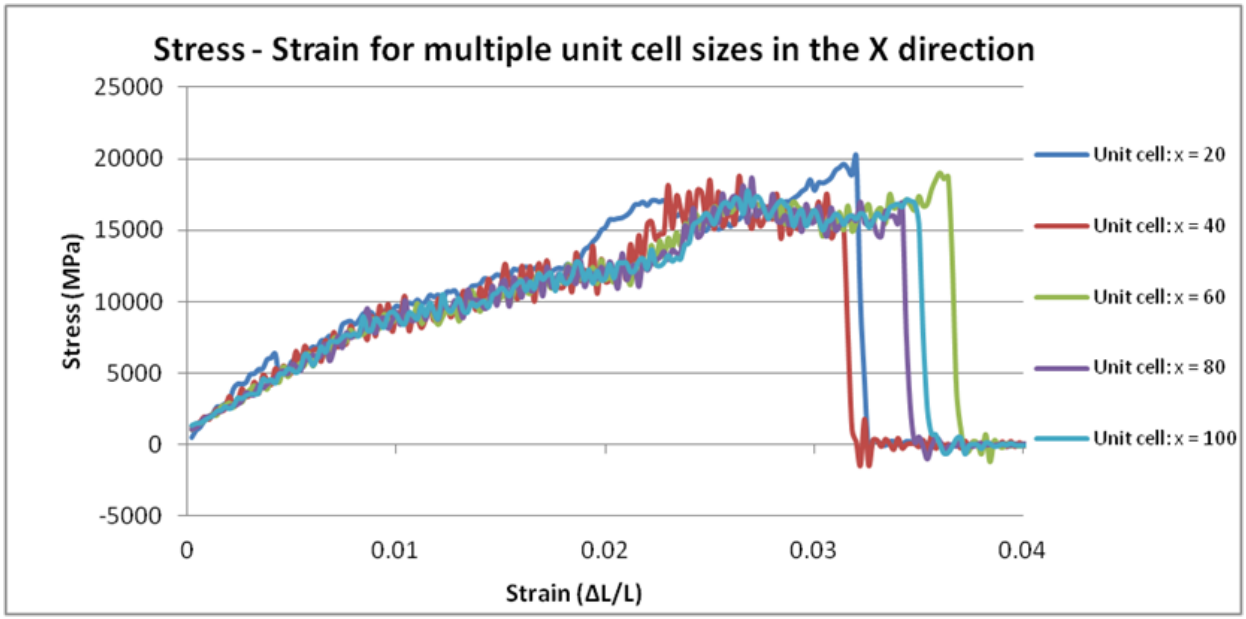

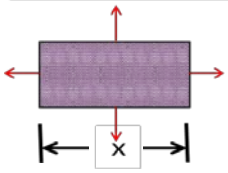

Figure 7. Stress vs. Strain response for single layer MoS2 with an increasing length (x direction). The image to the left shows the expansion in the x direction and the direction of loading on the system.

initial loading technique involved creating a strain on the system by giving these two fixed regions velocities equal and opposite of eachother.

In order to find the most suitable length for the simulations, the size of the lattice for the first simulation had a lattice length of 20 unit cells, or about 65Å, and was increased the length by multiples of 20 ending at 100. A biaxial load was applied to the lattice with a strain rate of 10^8. In order to simplify both the size of the simulation and the results, a single layer of MoS_2 was used. Conceptually, as the lattice thickness increases, the system also increases in complexity. Therefore, all simulations regarding boundary conditions in both the x and y directions used only a single layer. The results from each of the simulations were imported into Microsoft Excel and plotted on the same graph, shown in Figure 7. The most appropriate boundary conditions were taken visually from the median of lines in the graph, not the median in length.

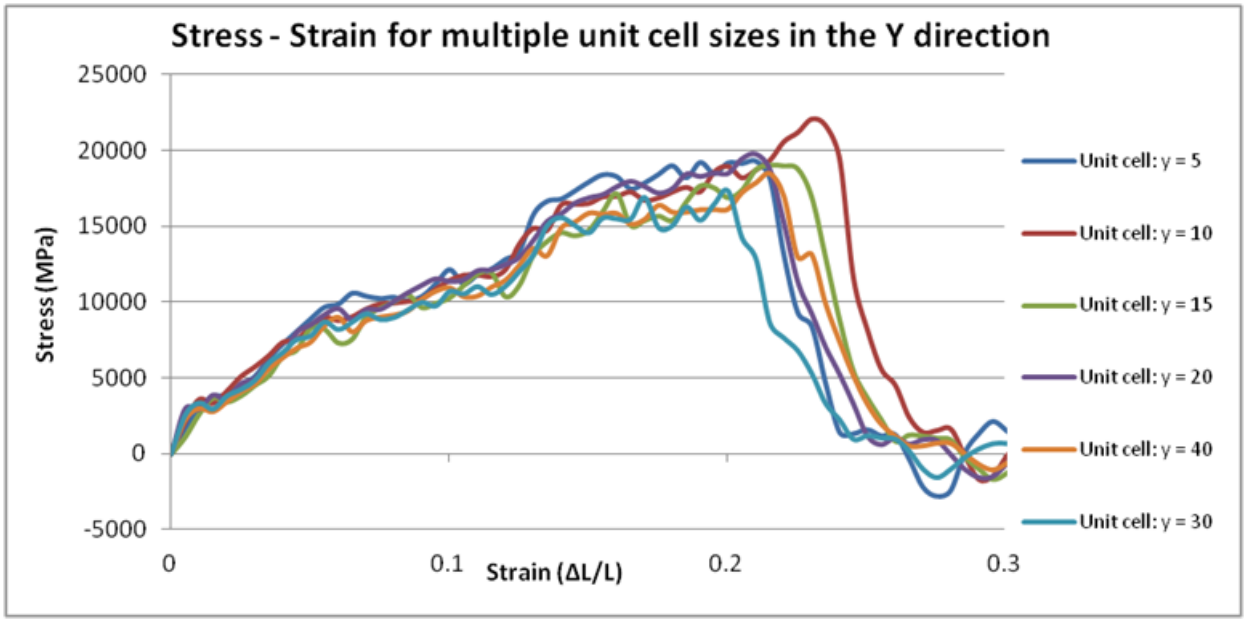

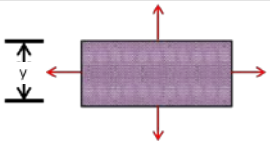

Figure 8. Stress vs. Strain response for single layer MoS2 with an increasing width (y direction). The image to the left shows the expansion in the y direction and the direction of loading on the system (Arrows).

Observations were made noting that the middle value, in terms of length of the lattice, was not always the median on the graph and sometimes ended up being either one of the two extremes.

In order to find the most suitable boundary conditions for the width of the lattice, simulations began with a lattice length of 80 unit cells, or about 260 angstrom. This set of simulations started with 5 unit cells in the y direction, or about 28 angstroms, and increased to 40 unit cells wide. The value for the suitable width of the lattice was again the median value was taken visually from the graph of stress - strain for the y direction, shown in Figure 8. After the analysis of this set of simulations was complete, research continued to the next set of simulations regarding the z direction, or thickness of the lattice.

The next step was to perform a set of simulations to find the proper boundary conditions for the thickness of the lattice. These simulations were different in the fact that instead of just increasing the size of the lattice, it actually introduces new layers to the system.

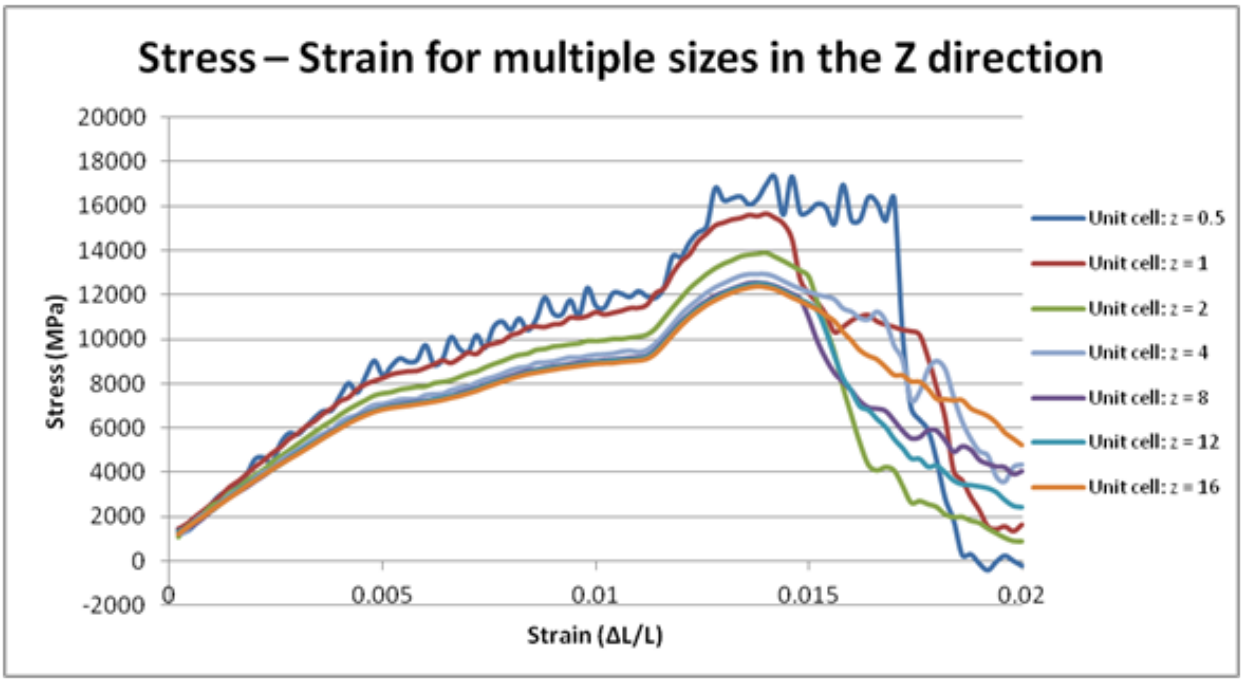

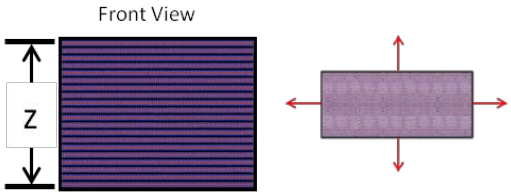

Figure 9. Stress vs. Strain response MoS2 with thickness varying from half a layer to 32 layers thick. The images to the left show the expansion in the thickness (or z direction) and the directions of loading on the system.

This means that by increasing thickness from a single sheet, or half a unit cell, of MoS_2 to 10 sheets, or 5 unit cells, the number of atoms in the system is increasing from 9,600 atoms to 96,000 atoms. The fact that the size of the system increases in such a drastic way is important due to the fact that this puts an increasing load on the supercomputers used to perform simulations. Therefore, finding an appropriate thickness for the lattice was the most important of the three boundary conditions being explored. Due to the extra loada that would have been put on the supercomputers, the strain rate used was twice that used for the simulation set finding suitable lengths for the system.

The stress vs. strain curves for the z directions are far smoother than that of the x and y directions, as seen in Figure 9. This was done by taking an average of three runs each of which started with a random thermal seed value resulting in a different random distribution of initial

velocities. The same three different seed values were used for each thickness of the lattice. The lattice in this set of simulations varied from 0.5 unit cells, or a single layer, to 16 unit cells. There were two main components of this graph that was observed. The first component was that as the thickness of the lattice of MoS_2 increased, the stress vs. strain curve began to converge to a consistent, predictable response. This means that after the thickness has increased to 20 layers, the system will react in a similar way to loading conditions. This consistent response could be classified as a bulk condition for this material. The second component that was observed was that the stress vs. strain curve differed from the typical curve seen in metals. The typical curve has two main components, or regions, that form the graph. Those two components are the elastic and plastic regions. The stress vs. strain curve shown above, as compared to that of metals, appears to have an elastic region, an unknown region, and an inelastic region. A problem cropped up during the process of analyzing the simulation during this middle region using Ovito. As the lattice thickness increases, visual analysis of the system became more difficult for the sole reason that there are too many failure occurring simultaneously. These failures can be seen in Figure 10.

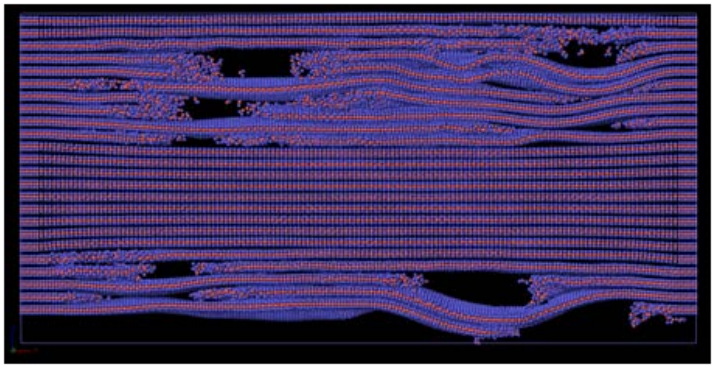

Figure 10. This image shows the complexity of a multi-layer system. In order to reduces this complexity, the thickness of the lattice is reduced to a single layer of MoS2.

The best way to simplify the system was to reduce the number of layers down to a single sheet and improve on the loading technique. A problem that was observed with the initial loading technique is that the directions with zero force did not contract proportionally with the change in length, as did the rest of the lattice. This resulted in a secondary force in the y

direction, in addition to the existing forces caused by the strain in the x direction. A few components of the input file had to be changed to create a pure uniaxial tension on the system. The first component was that the boundary in the x direction needed to be changed from non-periodic to periodic so that the boundaries for the simulation were periodic, periodic, and non periodic in the x, y, and z directions, respectively. The element that was required to be changed was the set of equations used to define the simulation, from the NVE ensemble to the NPT ensemble. Lastly was the implementation of a strain rate command in place of the velocities. This set of changes allowed for a specified strain rate to pull on the boundaries of the system instead of the lattice of MoS_2. This method allowed for the width to change proportionally to the length, as characterized by Poisson's ratio, and led to a pure uniaxial tension on the system. Next, simulations were run on the simplified system using the revised loading technique. The new stress vs. strain curve that resulted from the simplified simulation can be seen in Figure 11. This new loading technique used a strain rate of 10^9 and resulted in a much more pronounced second region. This indicates there must be a change in the physical make-up of the lattice during this region due to the law of conservation of energy. The main observation was that as the lattice continued to expand, the energy that was put into the system via the strain was not resulting in a change in stress. Therefore, this energy that is put into the system must have been put into changing the physical structure of the system.

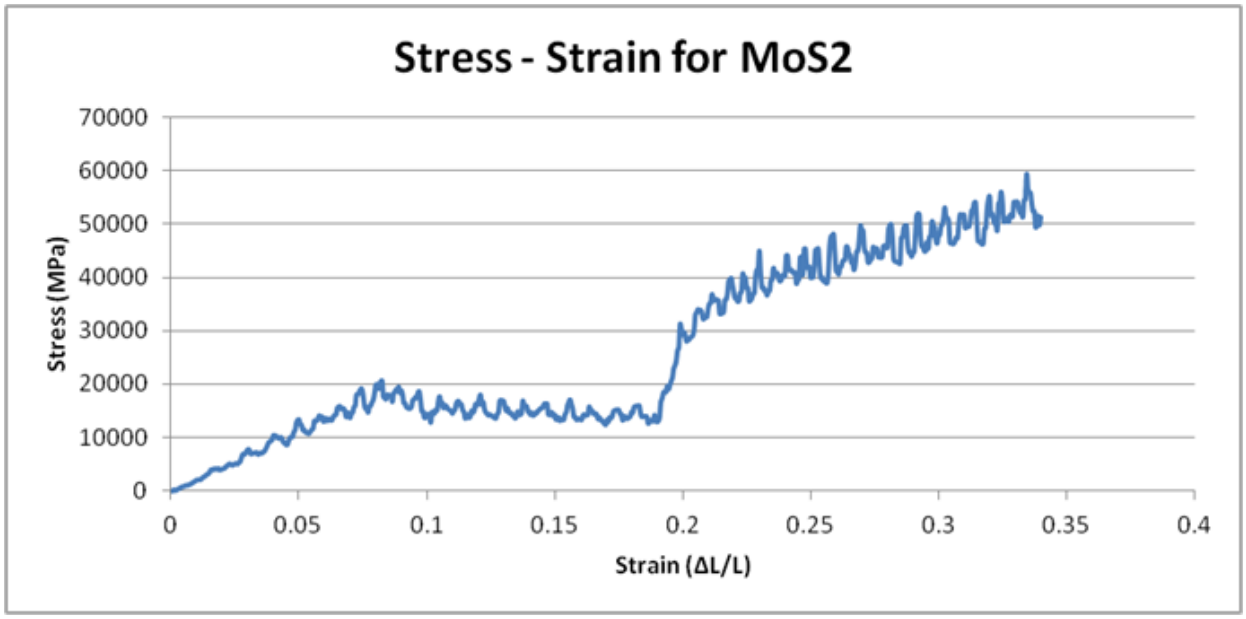

Figure 11. Stress vs. Strain response for single layer MoS2 under pure uniaxial tension. This images shows a more pronounced second region seen previously in Figure 9.

Next, the dump file associated with the simplified system was imported into Ovito in order to obtain a better understanding of what visually is happening throughout the course of the simulation. After being imported into OVITO, the lattice was color coded based on the potential energies of each atom. These potential energies were calculated at each time step in addition to many other variables. The images that were displayed showed the propagation of a new phase throughout the lattice of MoS_2 while the lattice continued to be stretched. The new phase filled the entire lattice and shortly after the lattice fractured. The propagation of the phase, as compared to the stress vs. strain curve of the single layer MoS_2 under uniaxial tension, can be seen in Figure 12.

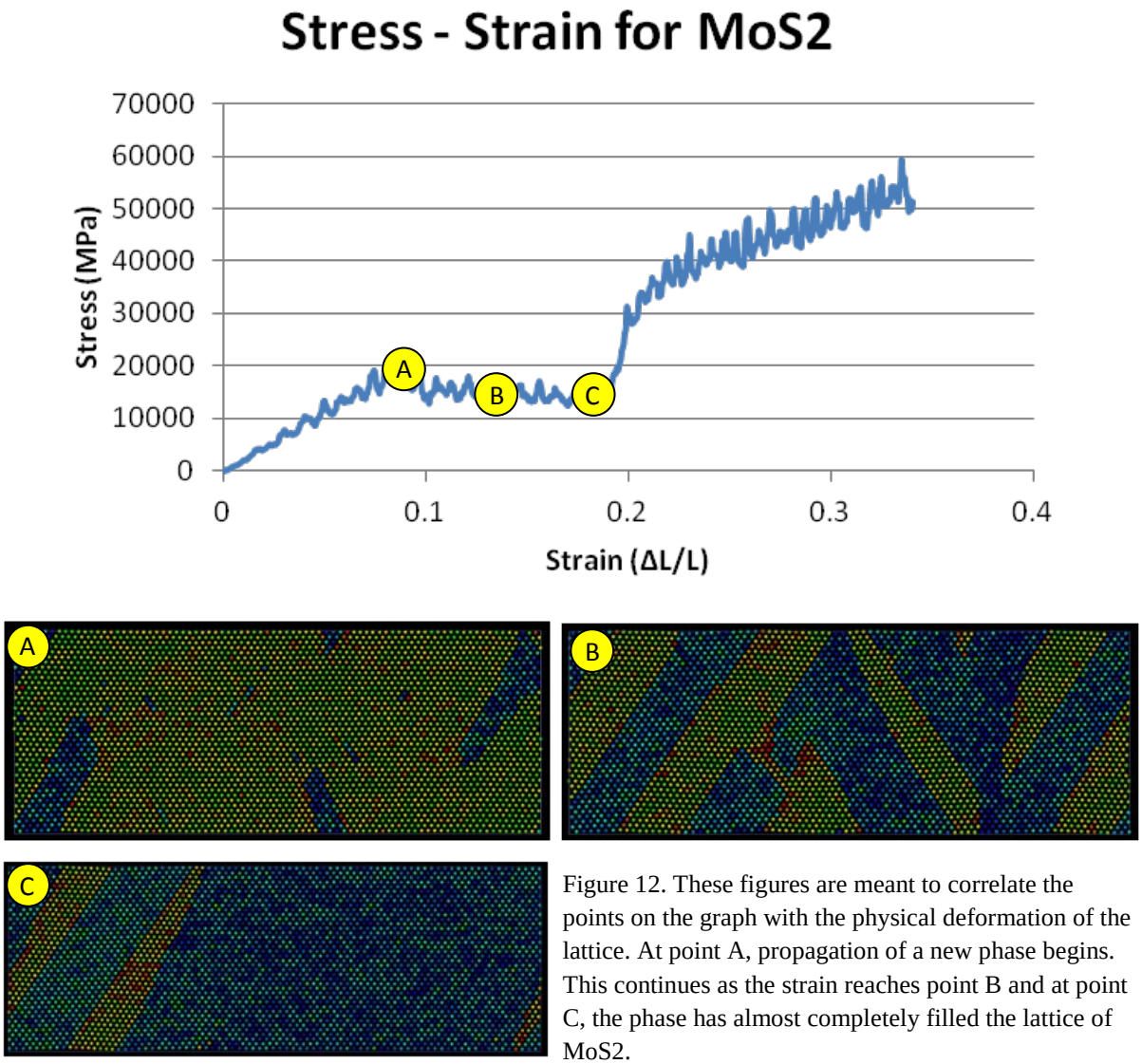

Figure 12. These figures are meant to correlate the points on the graph with the physical deformation of the lattice. At point A, propagation of a new phase begins. This continues as the strain reaches point B and at point C, the phase has almost completely filled the lattice of MoS2.

After this phase change had been observed, the new phase change was characterized and compared to literature. The first method employed to characterize the phase change was performing an overall system minimization. This process involved allowing the phase to propagate throughout the lattice of MoS_2, releasing the system from strain, performing a system minimization, and then calculating new lattice constants that could be used to recreate the lattice in another simulation. This method hypothesized that once the new phase had fully spread throughout the lattice, it had reached a new minimum energy configuration. This new energy configuration could then be brought back to zero strain and then evaluated. When

actually running through this process, the system rebounded back to the original composition, which had lattice constants of a = 3.17 Å and c = 12.29 Å, after the strain had been released. In addition to releasing it and performing a system minimization, the simulation was run until the system reached the middle second region, relaxed, and then pulled again until the lattice fractured. These simulations were performed specifically to confirm that the second region was a reversible deformation region in the stress vs. strain curve. The stress vs. strain curve shown in Figure 13 shows that when the system is run into the second region, released, and then allowed to run again, it acts in the same way as the initial run. Due to this fact, it was concluded that the second region is with a fully reversible plastic deformation of the lattice.

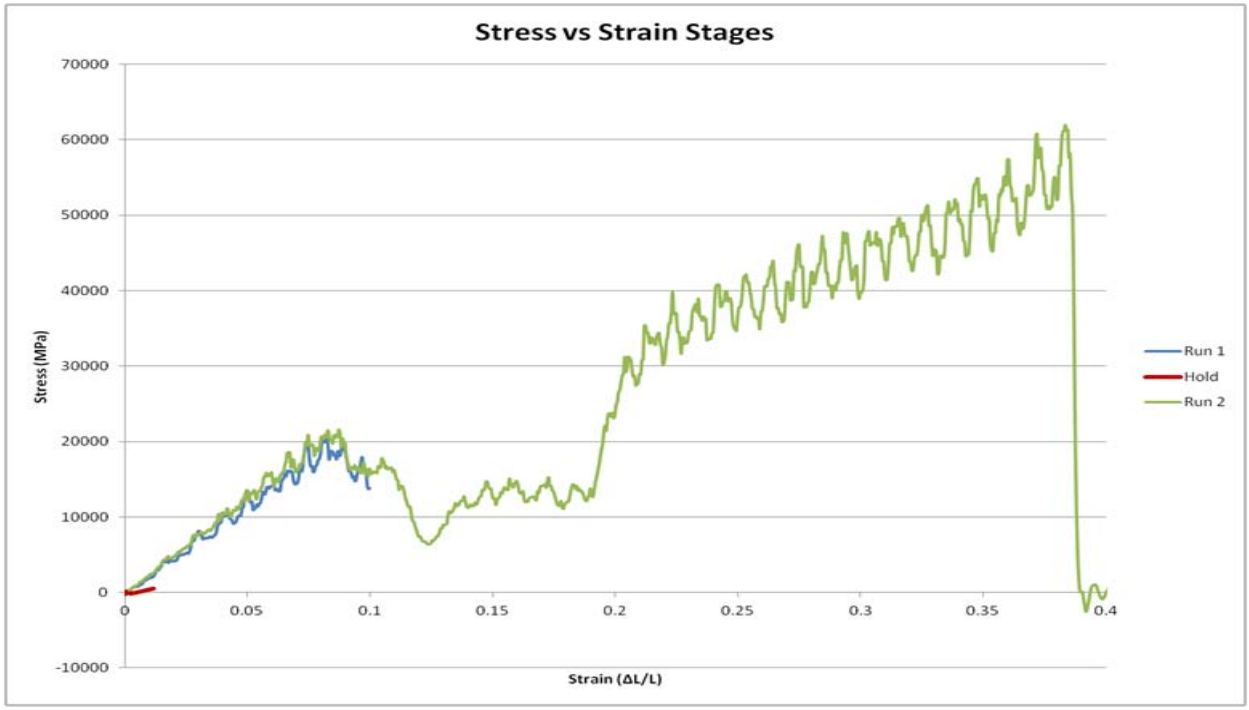

Figure 13. This graph shows a partial run into the second region, a release of the strain on the lattice. This release allows the strain on the system to return to zero at its own rate. After the strain has reached zero, a full run is performed. The two initial parts of each run are very similar in size and shape.

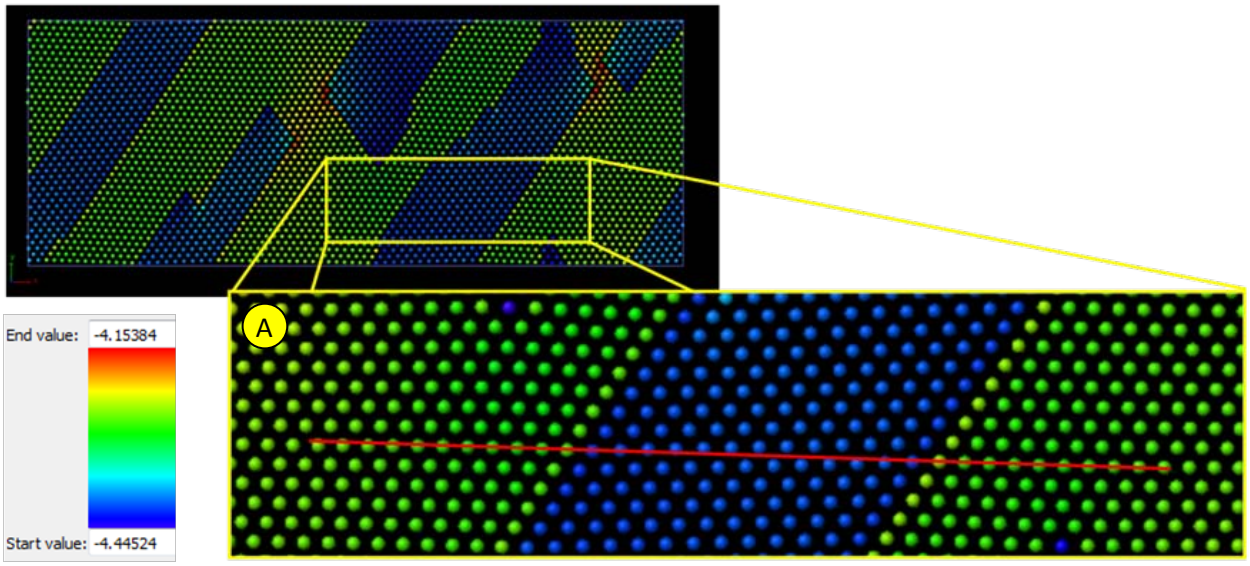

Figure 14. Zoomed in view (A) of the steepest decent minimization. The expanded view allows for visual analysis as a line is drawn from old phase (green) to old phase across the new phase (blue) that has propagated throughout the system. This lattice is color coded by potential energies with the units on the scale on the left side in electron Volts, or eV. (B) Shows a closer view, including the molybdenum atoms, of where the old and new regions meet.

The next minimization that was performed, a steepest decent minimization, was different in the fact that the energy minimum is attempting to find is a local energy minimum. The steepest decent minimization basically removes all thermal vibrations from the system and takes it down to zero degrees Kelvin. The main thing that was noticed when after viewing the steepest decent lattice was that there was some form of deformation due to the new phase. This steepest decent minimization allowed for a much clearer picture to be used for visual analysis of the deformation of the lattice due to the new phase. When zoomed in on a critical part of the lattice, the boundaries between the old and new phases, there appeared to be an even more apparent shift in the lattice. In order to help visualize what deformation was taking place, a line was drawn across the new phase, from old phase to old phase, along a line of atoms. The result of this

visual was an easily observed shift of one layer through the new phase. The same test was performed in almost every region of the lattice that had an old phase - new phase - old phase makeup. Every region acted in a similar way, a displacement of exactly one line of atoms.

Originally, the hypothesis behind the shift in the lattice was due to the formation of a line defect, this idea was proved wrong through the use of burgers circuits. A burgers circuit is used to analyze the area around a defect. If a lattice being analyzed by a burgers circuit has a dislocation inside of the circuit, the dislocation in the lattice can be characterized by a burgers vector. An example of this can be seen in Figure 15. The burgers vector looked promising due to the fact that it shows the size and direction of the lattice distortion due to the defect in the crystal structure. After numerous burgers circuits had been drawn, it appeared that the lattice was being deformed in the absence of bond breaking. This led to the next method of visual analysis.

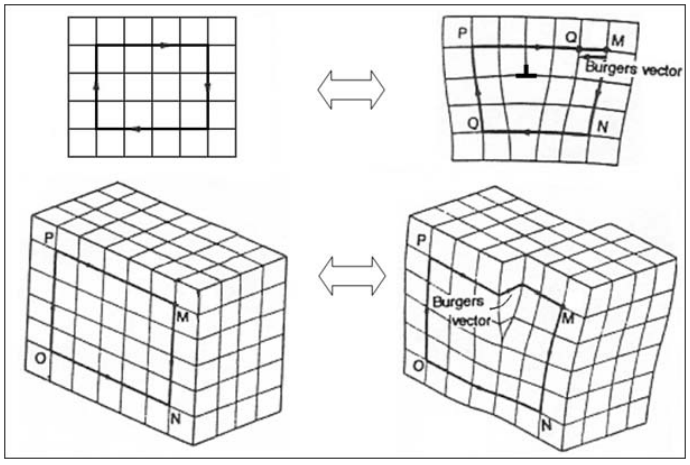

Figure 15. These are two examples of how a burgers circuit is used to characterize a defect in a lattice. [13]

There must be a physical distortion of the lattice due to the fact that the lattice was being deformed in the absence of breaking or formation of bonds. This method of visual analysis again used the steepest decent minimization and zoomed in even further than had been done previously. First, the positions of each atom in the hexagonal unit cells were recorded for both the old and new phases in the lattice, relative to a key central atom. Then the hexagonal unit cells were superimposed on top of one another centered on the central atom in each of the cells.

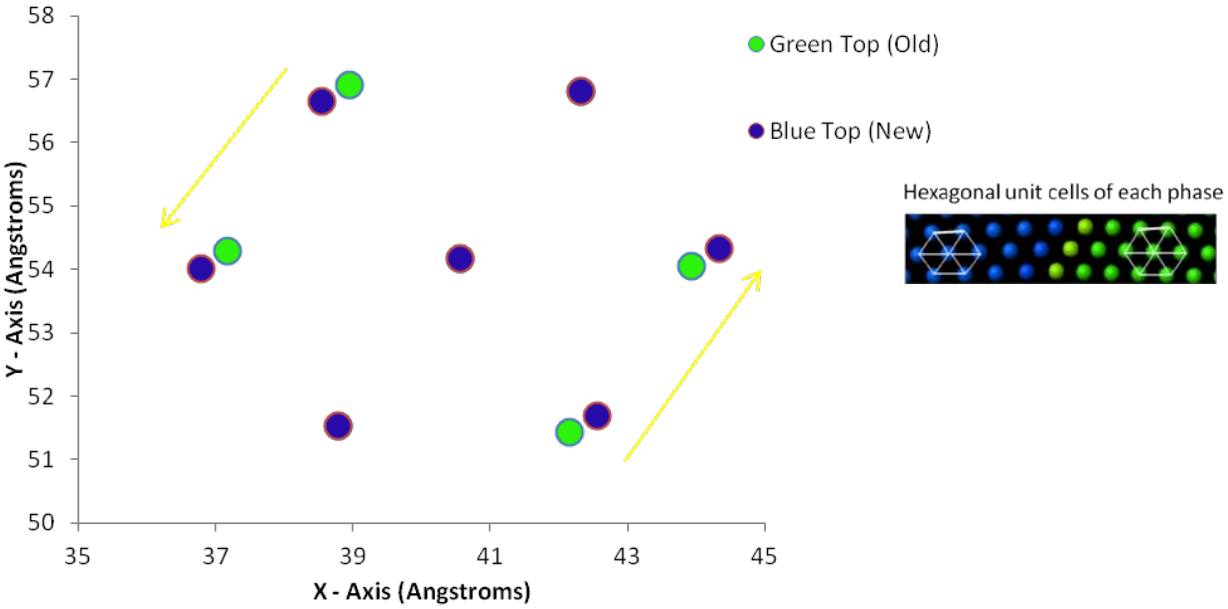

Figure 16. The upper right image shows the hexagonal unit cells of both the new phase (left) and the old phase (right). These hexagonal unit cells are superimposed, centered on the center atom. This allows for the visualization of specific displacements of each atom in the unit cell.

This allowed for a visual analysis of the specific displacements of each of the atoms in the unit cell.

It is apparent, using Figure 16, that the phase propagation throughout the lattice causes a shearing of the atoms. An observation from Figure 16 is the fact that there is a displacement of the atoms on the outer two diagonals, but no shift or shear appears to affect the inner diagonal. This is due to the diagonals shearing relative to each other with the distances between the atoms in each diagonal remaining the same. For example, if the unit cells were shifted over one diagonal, or one atom to either side, the middle diagonal in this figure would appear to have sheared in the next figure. This was validated by taking the positions of the two different phases and calculating the changes in distances, angles, and height of the atoms in the hexagonal unit cells. The results of this can be seen in Table 1.

		Distance			Angle			
	Atom - Atom	Green (Old)	Blue (New)	Difference	Angle	Green (Old)	Blue (New)	Difference
Outside	1-3	3.170	3.180	0.010	1-3-4 (A)	56.145	56.085	-0.060
	2-5	3.183	3.191	0.008	6-3-4	59.585	51.139	-8.447
	6-3	3.187	3.190	0.004	2-5-4	59.644	51.163	-8.481
	7-5	3.173	3.182	0.009	7-5-4	56.193	56.056	-0.136
Inside	1-4	3.186	3.190	0.004	1-4-3	59.587	51.135	-8.452
	2-4	3.170	3.181	0.010	6-4-3	56.196	56.062	-0.135
	6-4	3.173	3.182	0.008	2-4-5	56.124	56.083	-0.041
	7-4	3.184	3.192	0.007	7-4-5	59.637	51.173	-8.465
Horizontal	1-2	3.379	3.780	0.402	1-2-h	1.929	2.350	0.421
	3-4	3.381	3.779	0.398	3-4-h	1.951	2.354	0.403
	4-5	3.377	3.781	0.404	4-5-h	1.882	2.331	0.449
	6-7 (B)	3.380	3.779	0.399	6-7-h	1.916	2.334	0.418

h = horizontal

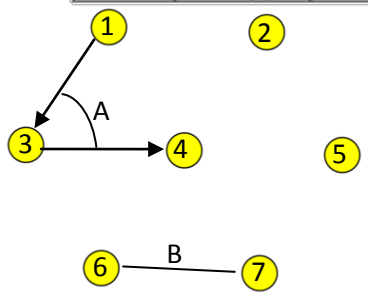

Table 1. The table above uses the hexagonal unit cells to quantitatively measure the differences between the two phases. The labeling system for the distance is from atom to atom and the labeling system for the angles in the lattice are atom 1 - atom 2 - atom 3. In the figure to the left, A) effectively demonstrates the labeling system for a 1-3-4 angle and B) shows an example for the distance between the atoms 6 and 7 (or 6-7).

This table shows the distances and angles for both the old and new phases. One observation of the table above is that the horizontal distances, between the 1 - 2 atoms for example, are increasing while the diagonal distances, between the 2 - 4 atoms, remain the same. Another observation is that angles such as the 6-3-4 angle are significantly reduced. This angle, and others like it, that have the two outside atoms of the angle on the same diagonal that goes from lower left to upper right, are all getting smaller. All of these observations confirm that the diagonals in the lattice are shearing relative to each other, without the separation of bonds, in order to find a new energy minimum under the effects of a tension. For example, if the left diagonal in the lattice shifted downward, the 6-3-4 angle would get smaller.

3.2 Exploration into Properties of Line Defects

Now that a lattice of sufficient size had been found, research into the effects of a defect on a lattice of MoS_2 could be started. The first step in research into line defects in an otherwise

perfect lattice of MoS_2 was to create a line defect. In order to create this line defect, a half plane of MoS_2 was deleted in the middle of the lattice, shown in Figure 17. Once this plane was gone there was a void where that layer should have been. There were three different method used to close this void. The first method used the “fix drag” command in LAMMPS to move the top down and the bottom upwards. This process moves every atom in a specified group towards a desired location and removes the force when it is closer than a specified distance away from the location. This method involved creating two groups, one directly above and one directly below the void. These two layers were moved together to fill this void. When the two groups moved together to fill the void, they cleanly broke apart from the rest of the layers. After running the simulation for a long equilibrium, the layers that had broken began to reform back into the original sheets of MoS_2 without any complications. The main problem with this method is after a long run time, the system was not stable and therefore another method had to be implemented. The second method used to fill the void was similar to the first, but this method used a "fix move" command to move the layers to the left of the defect in a similar fashion. The main difference between these two commands is the fact that with the first method, the atoms not affected by the command remain frozen and do not interact with the specified groups. This is the reason the sheets of MoS_2 cleanly break during the "fix drag" command. When running the script for the second method,

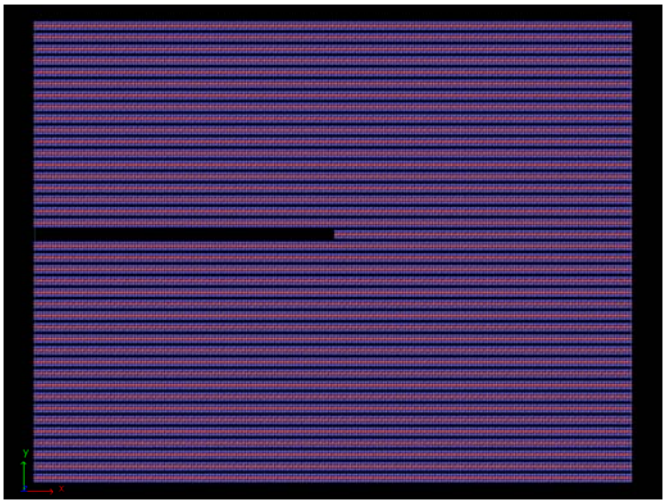

Figure 17. The image above shows the deletion of a half plane of MoS2 and the resulting void caused by this deletion.

all atoms are interactive while the "fix move" command is being carried out. Therefore, when the layers moved together to fill the void, they moved and stayed intact. Although this method appeared to have filled the void, after a long equilibrium the system again was not stable. Analysis of these first two methods led to a conclusion that the main problem, which led to the system being unstable, was the fact that there was no containing force or pressure that would lead to a stable system. This led to the final method used to create a line defect.

The third and final method used the same command as the second method, but with a different approach. Both the first and second methods used the "fix drag" and "fix move" commands on only the left half of the lattice above and below the defect. For this last method, the force on the top and bottom two layers were to zero. This freezes the atoms in the configuration and causes them to act like a rigid sheet. The "fix move" command was used on the top and bottom layers that had been frozen and in order to move them towards each other. This caused a slight compression of the entire lattice and also led to the top and bottom layers creating a containing force for the system. After some experimentation, an acceptable distance was found for the top and bottom layers to move that allowed the void in the lattice to close. After running the simulation for a long equilibrium, the system was very stable and the defect had

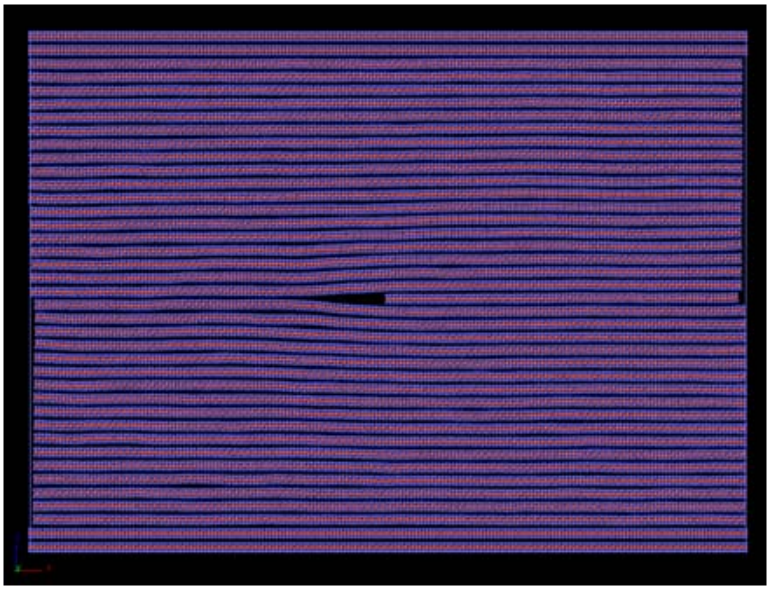

Figure 18. The image above is the final result in many attempts to close the void cause by deletion of a half plane. This lattice remained stable after an extended equilibrium.

been successfully been created, as shown in Figure 18. The theory behind this method is that when MoS_2 is used in applications as a solid lubricant, it will experience compressive forces. This method uses the minimum compressive force required for the system to reach a stable equilibrium while including a line defect.

An interesting side effect was the computational process used to determine how far the top and bottom should compress. An initial simulation had an over compressed lattice that caused defects to nucleate from the initial line defect as shown in Figures 19A, B, and C. Once

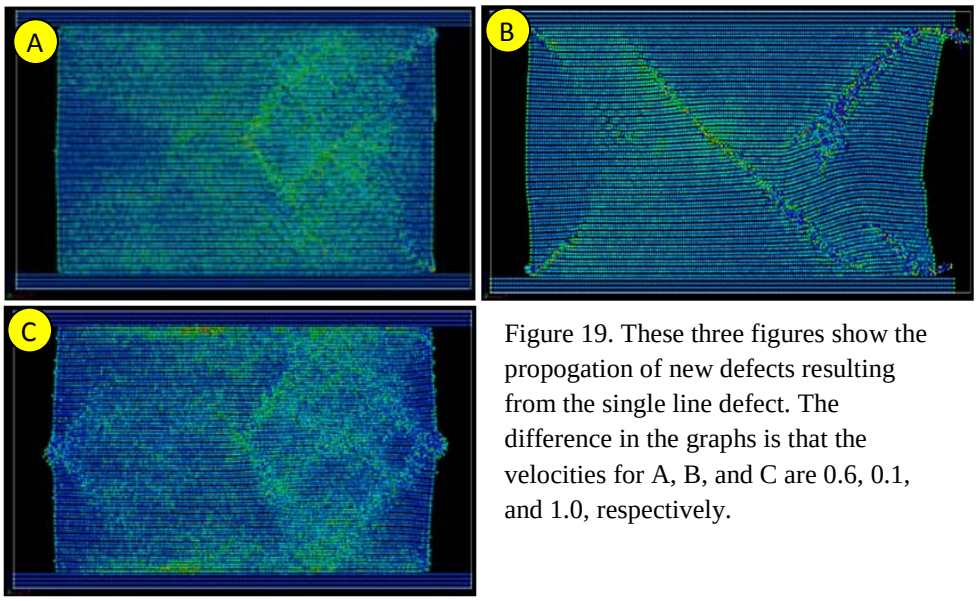

Figure 19. These three figures show the propogation of new defects resulting from the single line defect. The difference in the graphs is that the velocities for A, B, and C are 0.6, 0.1, and 1.0, respectively.

this was discovered, research started into how new defects nucleate from the line defect in the center of the lattice. Numerous simulations were run with velocities of 0.1, 0.2, 0.3, 0.4, 0.5, 0.6, 0.7, 0.8, 0.9, 1, 1.5, and finally 2 Å/ps. These simulations produced very interesting results. When compressed at different velocities, the lattices would fracture in different ways. These different reactions can be seen above in Figure 19.

The next step in the research was to attempt to move the defect through the lattice of MoS_2. There were two basic methods used to move the defect throughout the lattice. The first

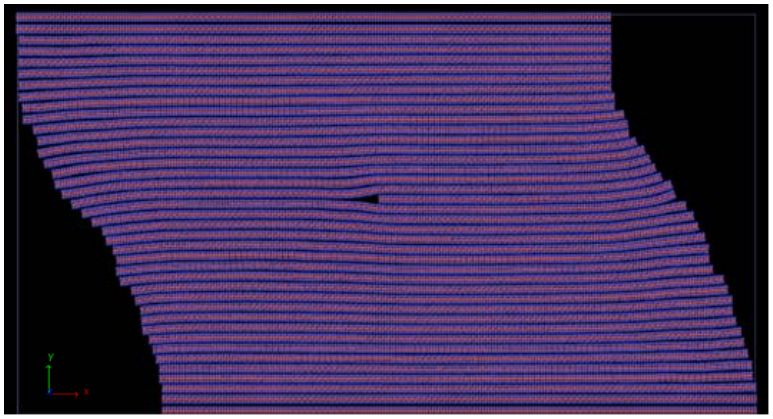

Figure 20. Shear of an MoS2 lattice with an additional ramp included in order to allow the lattice to move with the shear.

was to shear the system and the second was to create buckles in which the lattice would break and reform moving the defect up or down.

The first method involved shearing the top layer in either direction. The bottom layer was kept fixed while a velocity was created on the top layer oriented in the positive x direction. As expected, only the layers with the velocity command acting on them moved and the other layers remained in place. Next a velocity ramp was added to the lattice. The "velocity ramp" command in LAMMPS scales the velocity, vlow to vhigh, from ylow to yhigh. Basically the bottom has the velocity vlow, halfway through the lattice has the average of vlow and vhigh, and the top of the lattice has the velocity vhigh. This command creates a uniform movement throughout the lattice in one direction. The same process was repeated by creating a ramped velocity in the negative x direction, the results can be seen in Figure 20. After performing these simulations with numerous different velocities, a different approach to shearing was explored. After the lattice was

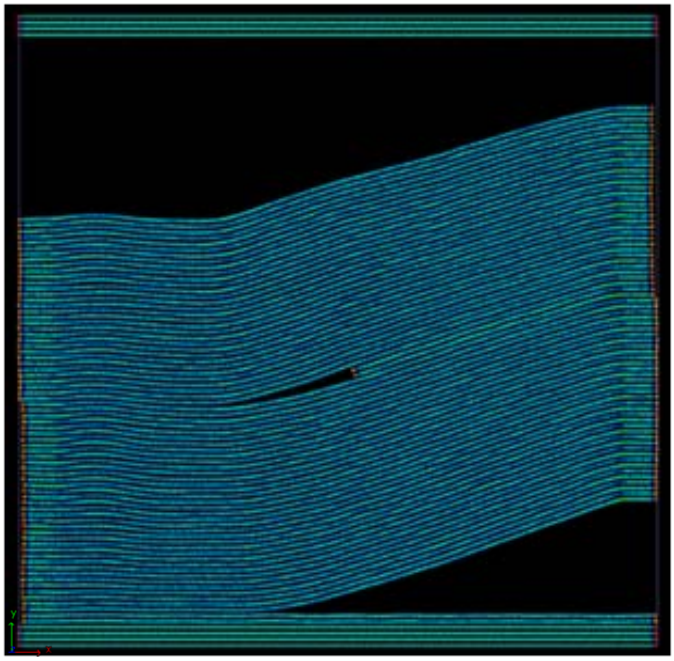

Figure 21. Shear in the z direction. This resulted in a fracture at the edges where the forces were zero. This was the precursor to the buckle method.

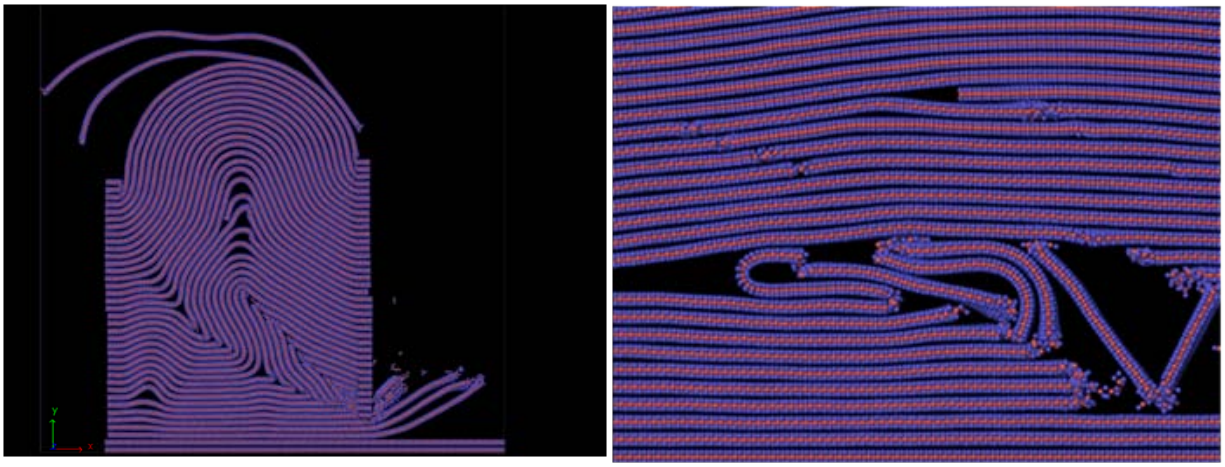

A B

Figure 22. The image on the left was the final attempt to move the line defect throughout the lattice. The buckling of the lattice allowed for the layers to break and reform (shown in B), but the entire process was too chaotic.

created, a velocity in the positive z direction was applied to the right five unit cells of the lattice while keeping the left side fixed in its position after the equilibration, as shown in Figure 21.

The shearing in the positive z direction was the predecessor for this next method. This method involves creating buckles, as shown in Figure 22A. After the buckles are created, the next step is continuing to compress the buckles, causing the layers to break, as shown in Figure 22B. In theory, when the buckles collapse, the layers will reform with new layers causing the defect to move. The first approach was to move the right five unit cells in the positive z direction, then move it to the upper left. This compresses the lattice in the x direction causing buckles to form. Then, the right side was moved straight down and then right, back to its original position. After the simulation was done running, there were completely broken layers and also partially broken layers that were beginning to reform. The problem, however, is that the layers did not break next to the initial line defect. In order to control where the layers break apart, the center of the original lattice with the defect already created was moved upward, in the positive z direction, while the lattice was compressed from the left and right sides towards the

center. This caused the layers to break in line with the defect. This has been the most promising method so far.

Finally, the strength of the lattice due to temperature variation was explored. All simulations to this point had been run at room temperature, the theory was that the covalent bonds in the lattice would become weaker with increasing temperature. This required the return to the stress strain curves used to find the suitable boundary conditions. Simulations were performed with the temperature for the system ranging from room temperature up to an extreme of 1200 °C. The results of the simulations can be seen below in Figure 23.

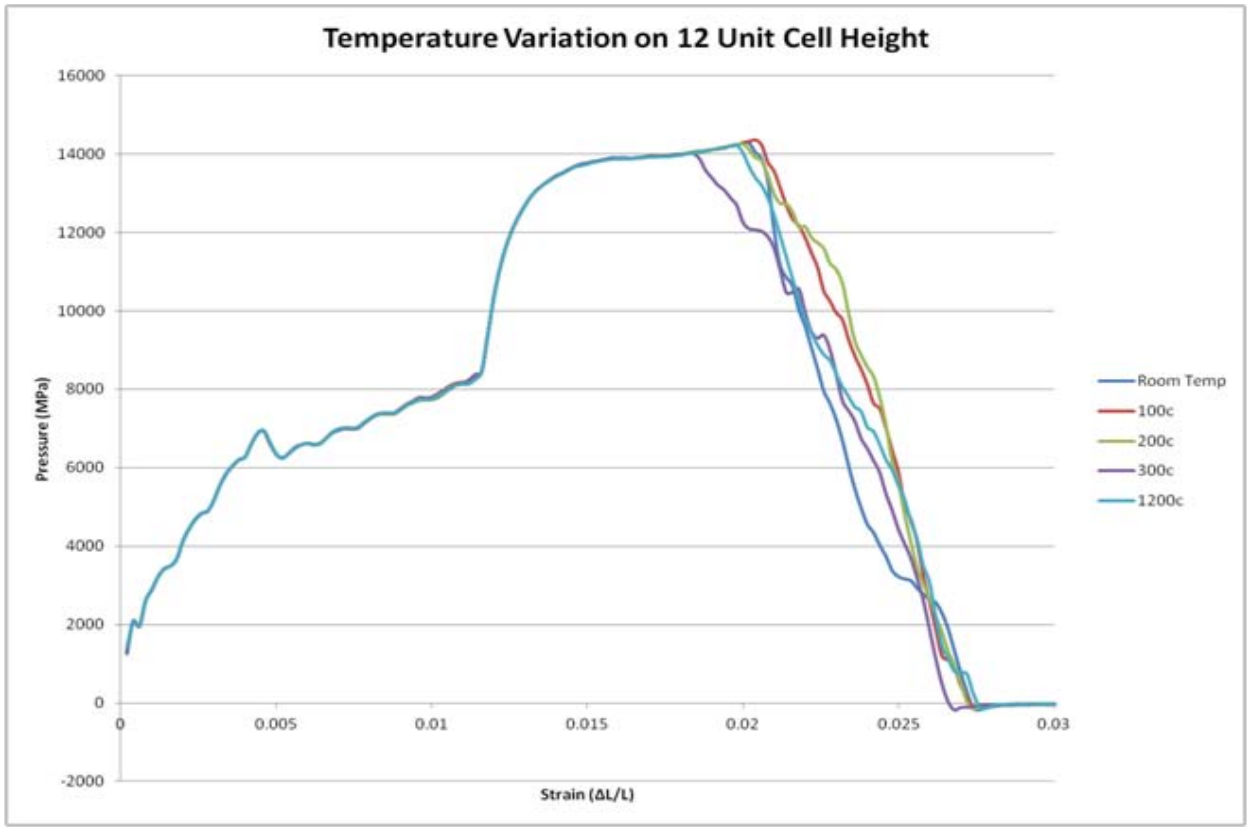

Figure 23. Stress vs. Strain response for 12 unit cell thick MoS2 with varying temperatures ranging from room temperature to 1200 degrees Celsius.

The graph shows that the variation of temperature on the lattice did not affect the strength of the bonding at all. The stress vs. strain responses for each of the temperatures is identical for most

of the simulation. This led to the conclusion that temperature variation would not affect the research into exploration into line defects in a lattice of MoS_2.

4.0 Conclusions

Although the majority of this research was intended to be focused on the properties of the defect in the lattice of MoS_2, the path to get to that point also proved fruitful. It was found that by increasing the size of the lattice, it will start to approach a bulk condition. This is important due to the fact that it was important information needed to create the appropriate size of a lattice in order to introduce the line defect. An unusual three region stress vs. strain curve was observed in Figure 9. This varies from the typical stress vs. strain curve in that the usual curve has two distinct regions: the linear elastic region and a non-linear non-elastic (or plastic) deformation region. If the curve for MoS_2 partially follows that of the typical curve, it appears to have a linear elastic region, an unknown region, and a non-linear plastic deformation region. In order to study this second unknown region, both the system and loading techniques were simplified to reduce as many variables as possible. The result was again a three region curve, but with a more pronounced second region. In order to investigate the properties of the second region, which now appeared as a plateau, the dump file that contained the entirety of the simulation was imported into Ovito. Each atom in the system was color coded by their potential energies.

This method of visual analysis clearly showed a propagation throughout the existing lattice of MoS_2 and then the fracture of the lattice. The critical points on the stress vs. strain curve were then correlated to the physical deformation of the lattice and found that the first peak, which immediately precedes the second region, was the initial point of propagation of a new phase. It was observed that the new phase propagates throughout the lattice entirely during the

second region and the simulation then proceeds similar to a typical stress vs. strain curve. At this point, there were a few conclusions to be made. The first is that the new phase propogates throughout the region in the absence of bond breaking. This can be seen by drawing burgers circuits around the new phase. The second conclusion is that it is a stress induced phase change, due to the fact that after releasing the lattice and letting it approach zero strain, the composition rebounds to the original phase. Another conclusion that was reached after simulations of reloading was that the second region must be a completely reversible plastic region. The simulations that were performed ran the strain into the second region, relaxed the system, and then performed an entire run. There was no drastically apparent difference in the behavior before and after the initial loading.

Although the efforts to create a mobile defect were futile, there were still a few observations to be made. The initial method of creating the line defect and compressing the lattice was valid. This is due to the main use for MoS_2 being a solid lubricant and as such, it would experience even small compressive forces. After attempting to move the defect throughout the lattice, multiple methods showed that the defect is immobile in the sense of moving up or down layers in the lattice. This is a result of the lamellar crystal structure and shows why it is a very useful material for solid lubrication. When attempting to move this defect through many varieties and applications of shear, the van der Waals bonds broke before the covalent bonds and allowed for the layers to slide parallel to each other. The last area of research was the variation of strength of the lattice with temperature. A conclusion was made that an increase in temperature has no adverse effects on the lattice and that the stress vs. strain curves for every temperature, ranging from room temperature to 1200 °C, were nearly identical

up until fracture. Through all of these simulations, it became apparent a line defect in MoS_2 will not move, or transfer, between the layer adjacent to it.

References:
[1] Stewart, James A., and Douglas E. Spearot. "Atomistic Simulations of Nanoindentation on the Basal Plane of Crystalline Molybdenum Disulfide (MoS_2)." *Modelling and Simulation in Materials Science and Engineering* (2013): n. pag. Print.
[2] Shankara, A., Pradeep L. Menezes, K. R. Y. Simha, and Satish V. Kailas. "Study of Solid Lubrication with MoS_2 Coating in the Presence of Additives Using Reciprocating Ball-on-flat Scratch Tester." *Sadhana* 33.3 (2008): 207-20. Print.
[3] *Http://www.flickr.com/photos/29504544@N08/4353789580/in/set-72157623301402075*. N.p., n.d. Web. 8 Apr. 2013.
[4] "Solid Film Lubricants: A Practical Guide." *Solid Film Lubricants: A Practical Guide*. N.p., n.d. Web. 14 Mar. 2013.
[5] "» Blog Archive » MoS_2 Molybdenum Disulphide: The Future Is No Longer Silicon Based?" *RSS*. N.p., n.d. Web. 14 Mar. 2013.
[6] "GenevaLunch News » MoS_2 Offers Tiny Chips, with Huge Energy Savings, Swiss Find." *GenevaLunch News RSS*. N.p., n.d. Web. 08 Apr. 2013.
[7] Ercolessi, Furio. "A Molecular Dynamics Primer." (1997). Print.
[8] Liang, Tao, Simon R. Phillpot, and Susan B. Sinnott. "Parametrization of a Reactive Many-body Potential for Mo–S Systems." *Physical Review B* 79.24 (2009): n. pag. Print.
[9] Spearot, D.E., "Atomistic Calculations of Nanoscale Interface Behavior in FCC Metals," Ph.D. Dissertation, Georgia Institute of Technology, 2005.
[10] "LAMMPS Molecular Dynamics Simulator." *LAMMPS Molecular Dynamics Simulator*. N.p., n.d. Web. 08 Apr. 2013.
[11] "Hardware | Hpc.uark.edu." *Hardware | Hpc.uark.edu*. N.p., n.d. Web. 08 Apr. 2013.
[12] "OVITO - The Open Visualization Tool Scientific Visualization and Analysis Software for Atomistic Simulation Data." *Home*. N.p., n.d. Web. 08 Apr. 2013.
[13] *Http://upload.wikimedia.org/wikipedia/commons/5/57/Vector_de_Burgers.PNG*. N.p., n.d. Web. 8 Apr. 2013.